Temperature-Dependent Study of the $CH_3C(O)O_2$ + NO Reaction

M. Matti Maricq* and Joseph J. Szente

Research Laboratory, Ford Motor Company, P.O. Box 2053, Drop 3083, Dearborn, Michigan 48121

Received: March 14, 1996; In Final Form: May 7, 1996[⊗]

The kinetics of the reaction between acetylperoxy radicals and nitric oxide have been examined both by transient IR absorption and by time-resolved UV spectroscopy. The former technique enables measurements of NO loss and NO_2 formation, whereas the latter provides data on the decay of acetylperoxy radicals, the secondary formation of methylperoxy radicals, and their conversion into methylnitrite. The two methods give consistent rate constants which are fit by the expression $k_1 = (2.1^{+1.4}_{-0.8}) \times 10^{-12} e^{(570\pm140)/T}$ cm^3 s^{-1}. The room temperature value of $k_1 = (1.4 \pm 0.2) \times 10^{-11}$ cm^3 s^{-1} is somewhat smaller than the currently recommended value, which is based on indirect determinations of k_1. Measurements of the CH_3O_2 and NO_2 yields indicate that the reaction proceeds exclusively to the products $CH_3C(O)O$ and NO_2. The negative temperature dependence suggests that the reaction proceeds via an intermediate adduct that rearranges and dissociates into the products.

I. Introduction

Peroxyacetylnitrate (PAN) is a ubiquitous compound found in photochemical smog. It originates from the atmospheric degradation of acetaldehyde, acetone, and methylglyoxal, as well as other compounds that produce acetylperoxy radical as an intermediate in the degradation process. The association reaction between this radical and NO_2 forms PAN. This is a relatively stable adduct that sequesters NO_2. In so doing, PAN provides a mechanism for the long-range transport of NO_x, in particular from urban areas with relatively high NO_x concentrations to rural areas where they are naturally much lower.

The formation of PAN, however, is not the sole fate of the acetylperoxy radical; it can also react with NO, HO_2, or other peroxy radicals, such as CH_3O_2.[1] In contrast to PAN formation, which sequesters NO_2, the reaction

$$CH_3C(O)O_2 + NO \rightarrow CH_3C(O)O + NO_2 \qquad (1)$$

converts nitric oxide to NO_2. Peroxy radicals typically react rapidly with NO. Photolysis of the NO_2 that they produce regenerates nitric oxide and releases atomic oxygen. The latter subsequently combines with molecular oxygen and, thus, is a source of tropospheric ozone.

To date, information about the reaction between acetylperoxy radicals and NO has come from indirect measurements that are based on observing the decomposition rate of PAN as a function of [NO]/[NO_2]. They provide a rate constant ratio, k_{NO}/k_{NO_2}, in the range of 1.9−2.4 that is insensitive to temperature.[2−5] When this ratio is combined with the recommended value of the rate constant for the reaction

$$CH_3C(O)O_2 + NO_2 + M \rightarrow CH_3C(O)O_2NO_2 + M \qquad (2)$$

one obtains $k_1 = (1.9 \pm 1.0) \times 10^{-11}$ cm^3 s^{-1} independent of temperature over the 283−328 K range.[6]

The present paper reports the results of a direct investigation of the $CH_3C(O)O_2$ reaction with NO over the 228−354 K temperature range. Measurement of the rate constant for reaction (1) is complicated by the significant secondary chemistry that occurs subsequent to this reaction, namely

$$CH_3C(O)O \rightarrow CH_3 + CO_2 \qquad (3)$$

$$CH_3 + O_2 + M \rightarrow CH_3O_2 + M \qquad (4)$$

$$CH_3O_2 + NO \rightarrow CH_3O + NO_2 \qquad (5)$$

$$CH_3O + NO + M \rightarrow CH_3ONO + M \qquad (6a)$$

$$CH_3O + NO \rightarrow CH_2O + HNO \qquad (6b)$$

Consequently, we felt that it would not be possible to make a reliable determination of k_1 simply on the basis of observing the change in concentration of any single species. Instead, transient IR absorption is used to measure the loss of NO from reactions (1), (5), and (6) and the formation of NO_2 via reactions (1) and (5). The loss of $CH_3C(O)O_2$, its conversion into CH_3O_2 by reactions (3) and (4), and the formation of CH_3ONO by reactions (5) and (6a) are measured by time-resolved UV spectroscopy. That consistent results are obtained lends confidence that the measurement of k_1 is as free as possible from the effects of the secondary chemistry.

II. Experimental Section

The experimental techniques are the same as described previously for the ethylperoxy reaction with NO and to which the reader is referred for detail.[7] Briefly, acetylperoxy radicals are generated in a flowing $Cl_2/CH_3CHO/NO/O_2/N_2$ gas stream by the 351 nm excimer laser photolysis of Cl_2 and the reactions

$$Cl + CH_3CHO \rightarrow CH_3CO + HCl \qquad (7)$$

$$CH_3CO + O_2 + M \rightarrow CH_3C(O)O_2 + M \qquad (8)$$

A ~300 mJ laser pulse generates (5−15) × 10^{14} cm^{-3} radicals in a probe volume measuring roughly 0.8 cm in diameter and 51 cm in length. The quantities of acetaldehyde (~2 Torr) and O_2 (>20 Torr) are sufficient to ensure that the photolyzed chlorine atoms are converted to peroxy radicals on a 200 ns timescale ($k_7 = 7.5 \times 10^{-11}$ cm^3 s^{-1}, $k_8 = 5 \times 10^{-12}$ cm^3 s^{-1})[8].

NO and NO_2 concentrations are monitored by transient diode laser absorption using vibration−rotation lines of the $v = 0 \rightarrow 1$ transition of NO at 1850 cm^{-1} and the ν_3 asymmetric stretch of NO_2 at 1630 cm^{-1}. The transient changes in absorption, $I(t)$,

---

* Author to whom correspondence should be addressed.

[⊗] Abstract published in *Advance ACS Abstracts,* June 15, 1996.

S0022-3654(96)00792-7 CCC: $12.00

are converted to concentration versus time profiles via

$$[X]_t = \frac{1}{\sigma_X l} \ln\left(\frac{I_b + I(t)}{I_0}\right) \qquad (9)$$

where l is the path length, σ_X is the IR absorption cross section of species X, and I_0 is the diode laser intensity. I_b is the transmitted intensity of the gas mixture prior to photolysis, which must be added to the transient intensity change because the HgCdTe IR detector operates as an ac coupled device. The required IR cross sections, which are temperature and pressure sensitive, are measured separately for each experiment.

Time-resolved UV spectra of the reaction mixture are obtained by passing broad-band light from a D_2 lamp through the reaction cell, dispersing the light with a monochromator (at ~3 nm resolution), and detecting it with a gated diode array (~4 μs time resolution). Fitting these spectra to the expression

$$Abs(\lambda,t) = \sum_i l\sigma_i(\lambda)\, C_i(t) \qquad (10)$$

furnishes the changes in the $CH_3C(O)O_2$, CH_3O_2, and CH_3ONO concentrations with time. Here l is the path length, $\sigma_i(\lambda)$ is the wavelength-dependent cross section of species i and $C_i(t)$ is its time-dependent concentration. As is described below, these fits are complicated by the presence of additional, but minor, UV-absorbing secondary products including $CH_3O_2NO_2$ and HNO. However, the measurements of $[CH_3C(O)O_2]_t$ and $[CH_3O_2]_t$ remain largely unaffected by the presence of these species. The reference spectra, $\sigma_i(\lambda)$, are obtained as follows: $CH_3C(O)O_2$, ref 9; CH_3O_2, CH_3ONO, and NO_2, ref 10; HNO and NO, ref 7; $CH_3C(O)O_2NO_2$ and $CH_3O_2NO_2$, present study.

The $CH_3C(O)O_2 + NO$ rate constant is determined by least-squares fits of the data to the reaction model presented below treating k_1 as an adjustable parameter. For the IR experiments, the NO and NO_2 data are simultaneously fit subject to an independently determined initial radical concentration; for the UV experiments the $CH_3C(O)O_2$ and CH_3O_2 data are simultaneously fit. For these overconstrained systems, agreement between model predictions and the data lends confidence to the reaction model and the measured rate constant.

Gas flows are set by Tylan flow controllers. Their concentrations are determined by measuring the pressure rise upon flowing them individually into a fixed volume. The temperature is controlled by a recirculating bath. The gas stream is prewarmed/precooled to the temperature setpoint prior to entering the reaction cell. Cl_2 (9.7% in He) and NO (10% in N_2) are obtained from Matheson. Comparison of the NO mixture against pure NO using difference IR spectroscopy verified the concentration at 10.2 ± 0.2%. N_2 (99.999%) and O_2 (99.6%, hydrocarbons < 0.2 ppm) are obtained from Michigan Airgas. CH_3CHO (99.5%) is obtained from Aldrich.

III. Results

TABLE 1: $CH_3C(O)O_2 + NO$ Reaction Mechanism

reaction[a]	rate constant
1. $CH_3C(O)O_2 + NO \rightarrow CH_3C(O)O + NO_2$	$k_1 = 2.1 \times 10^{-12} e^{570/T}$ $cm^3\ s^{-1}$ [b]
11. $CH_3C(O)O_2 + CH_3C(O)O_2 \rightarrow 2\ CH_3C(O)O + O_2$	$k_{11} = 3.0 \times 10^{-12} e^{504/T}$ $cm^3\ s^{-1}$ [9]
13a. $CH_3C(O)O_2 + CH_3O_2 \rightarrow CH_3C(O)O + CH_3O + O_2$	$k_{13a} = 0$
13b. $CH_3C(O)O_2 + CH_3O_2 \rightarrow CH_3COOH + CH_2O + O_2$	$k_{13b} = 8.5 \times 10^{-13} e^{726/T}$ $cm^3\ s^{-1}$ [9]
3. $CH_3C(O)O \rightarrow CH_3 + CO_2$	$k_3 > 1 \times 10^6\ s^{-1}$
4. $CH_3 + O_2 + M \rightarrow CH_3O_2 + M$	$k_4 = 4.5 \times 10^{-31}(T/300)^{-3}$ $cm^6\ s^{-1}$ [11]
5. $CH_3O_2 + NO \rightarrow CH_3O + NO_2$	$k_5 = 4.2 \times 10^{-12} e^{180/T}$ $cm^3\ s^{-1}$ [11]
12a. $CH_3O_2 + CH_3O_2 \rightarrow 2\ CH_3O + O_2$	$k_{12a} = (1 - b) \times 9.1 \times 10^{-14} e^{416/T}$ $cm^3\ s^{-1}$ [1]
12b. $CH_3O_2 + CH_3O_2 \rightarrow CH_3OH + CH_2O + O_2$	$k_{12b} = b \times 9.1 \times 10^{-14} e^{416/T}$ $cm^3\ s^{-1}$ $b = (1 + 25 \times e^{-1165/T})^{-1}$
6a. $CH_3O + NO + M \rightarrow CH_3ONO + M$	$k_6 = 3.6 \times 10^{-11}(T/300)^{-0.6}$ $cm^3\ s^{-1}$ [11]
6b. $CH_3O + NO \rightarrow CH_2O + HNO$	
2. $CH_3C(O)O_2 + NO_2 + M \rightarrow CH_3C(O)O_2NO_2 + M$	$k_2 = 9.3 \times 10^{-12}(T/300)^{-1.5}$ $cm^3\ s^{-1}$ [11]
14. $CH_3O_2 + NO_2 + M \rightarrow CH_3O_2NO_2 + M$	$k_{14} = 6.5 \times 10^{-11}(T/300)^{-2}$ $cm^3\ s^{-1}$ [11]
15. $CH_3O + NO_2 + M \rightarrow CH_3ONO_2 + M$	$k_{15} = 2.0 \times 10^{-11}$ $cm^3\ s^{-1}$ [11]
16. $CH_3 + NO + M \rightarrow CH_3NO + M$	$k_{16} = 1.7 \times 10^{-11}$ $cm^3\ s^{-1}$ [12]
17. $CH_3 + NO_2 + M \rightarrow CH_3NO_2 + M$	$k_{17} = 3.4 \times 10^{-11}$ $cm^3\ s^{-1}$ [12]

[a] Reaction numbers correspond to those used in the text. [b] Measured in the present study.

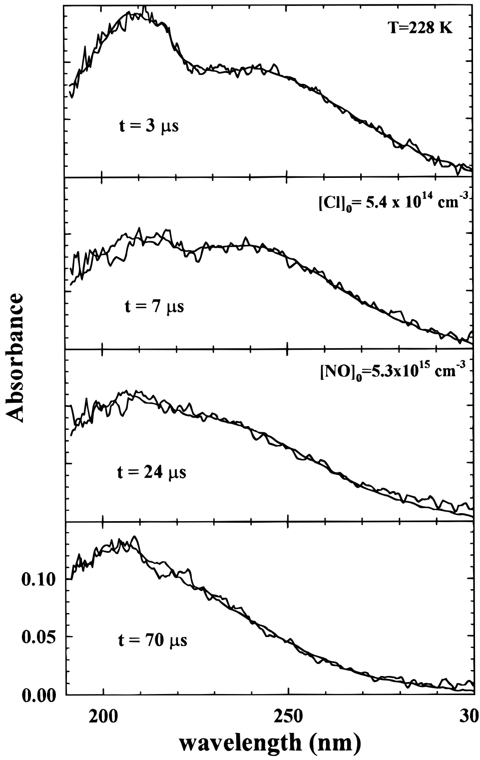

Figure 1. Time-resolved UV spectra of a $Cl_2/CH_3CHO/NO/O_2/N_2$ gas mixture at various times after Cl_2 photolysis at 351 nm. The smoother appearing lines represent fits of the absorbances to expression (10) with the concentrations of $CH_3C(O)O_2$, CH_3O_2, the CH_3ONO composite, and the peroxynitrate products treated as four fitting parameters.

a. Reaction Model. The photolysis of a $Cl_2/CH_3CHO/NO/O_2/N_2$ gas mixture initiates a sequence of chemical reactions beginning with reactions 7 and 8 and continuing with those detailed Table 1. The first two steps are set to be rapid by adjusting the concentrations of acetaldehyde and oxygen; thus, formation of acetylperoxy radicals is taken to be essentially instantaneous. The presence of this radical shortly after the photolysis pulse and its subsequent decay can be seen from the time-resolved UV spectra displayed in Figure 1. A comparison to the reference spectra presented in Figure 2 reveals that the absorbance of the reaction mixture at 3 μs arises predominantly from $CH_3C(O)O_2$. By 7 μs the reaction with NO has reduced the intensity of the band at 209 nm relative to the intensity of the 242 nm band. This is consistent with the decay of CH_3C-

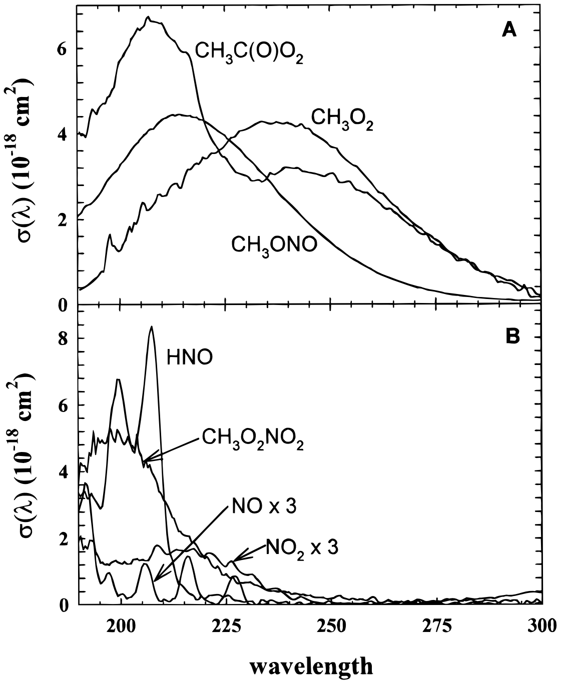

Figure 2. Reference spectra of species contributing to the total UV absorbance of the reaction mixture. Panel A shows the principal UV-absorbing molecules. Panel B shows the spectra of species considered minor either because they arise from minor secondary reactions or because their absorption cross sections are small. Not shown is the spectrum of $CH_3C(O)O_2NO_2$, which resembles very closely that of $CH_3O_2NO_2$.

(O)O_2 and the subsequent formation, via reactions (3) and (4), of CH_3O_2, which has only a single absorption band at 238 nm. Because the shape and intensity of the methylperoxy absorption is similar to that of the longer wavelength band of acetylperoxy (see Figure 2), the absorbance near 240 nm remains virtually unchanged. However, by 24 μs the absorbance at this wavelength has begun to decay owing to the loss of methylperoxy radicals, primarily via their reaction with NO. At the same time the intensity at short wavelengths, near 210 nm, has begun to increase again because of methylnitrite formation via reaction (6a).

In addition to these principal reactions, a number of others play roles in the chemistry of the reaction mixture. Except at low NO concentrations, most are of negligible consequence. First, acetylperoxy radicals are lost relatively rapidly by their self-reaction,

$$CH_3C(O)O_2 + CH_3C(O)O_2 \rightarrow 2CH_3C(O)O + O_2 \qquad (11)$$

a process that competes with reaction (1). Likewise, the methylperoxy radicals that are subsequently formed also undergo self-reaction

$$CH_3O_2 + CH_3O_2 \rightarrow 2CH_3O + O_2 \qquad (12a)$$

$$CH_3O_2 + CH_3O_2 \rightarrow CH_3OH + CH_2O + O_2 \qquad (12b)$$

albeit more slowly, and they can react with the parent acetylperoxy radicals

$$CH_3C(O)O_2 + CH_3O_2 \rightarrow CH_3C(O)O + CH_3O + O_2 \quad (13a)$$

$$CH_3C(O)O_2 + CH_3O_2 \rightarrow CH_3COOH + CH_2O + O_2 \quad (13b)$$

Each of the reactions (11)−(13) becomes less of a factor as $[NO]_0/[RO_2]_0$ increases. For the present experiments this ratio varies between 2.5 and 13.

Another class of secondary reactions involves those between the peroxy radicals, as well as CH_3O, and the NO_2 that is produced by reactions (1) and (5). This includes PAN formation, reaction (2), and the reactions

$$CH_3O_2 + NO_2 + M \rightarrow CH_3O_2NO_2 + M \qquad (14)$$

$$CH_3O + NO_2 + M \rightarrow CH_3ONO_2 + M \qquad (15)$$

Because $[NO_2] \leq 2[RO_2]_0$, these reactions, too, become less important as the $[NO]_0/[RO_2]_0$ ratio increases.

Although the methyl radicals liberated by the dissociation of $CH_3C(O)O$ primarily react with the O_2 present in the cell, this reaction is not particularly rapid. Thus, at the higher initial nitric oxide levels it becomes possible that some of the methyl radicals are lost by

$$CH_3 + NO + M \rightarrow CH_3NO + M \qquad (16)$$

Similarly, the reaction

$$CH_3 + NO_2 + M \rightarrow CH_3NO_2 + M \qquad (17)$$

contributes to the removal of methyl radicals, although to a much smaller degree than reaction (16) because $[NO_2] \ll [NO]$. Even at the highest $[NO]_0/[O_2]$ ratios employed in these experiments, >85% of the methyl radicals are expected to add oxygen to form CH_3O_2.

Finally, one could point out that regeneration of $CH_3C(O)O_2$ is conceivable due to OH radicals formed from the reaction of CH_3O with O_2 followed by the reaction of the HO_2 product with NO. Were this to happen, it would complicate the measurement of k_1. However, because of the small rate constant for its reaction with O_2, the methoxy radicals in these experiments are lost almost entirely via their reaction with NO and no regeneration occurs.

b. UV Measurements. Ideally the time-resolved UV absorbances are composed of varying contributions from absorption by $CH_3C(O)O_2$, CH_3O_2, and CH_3ONO, with the first compound dominating at early times and the last one at late times. In practice, the spectrum long after the photolysis pulse does not arise solely from the presence of methylnitrite. Small contributions, owing to the small optical cross sections of these molecules, arise from the loss of NO and the formation of NO_2. Furthermore, aside from their contributions to the kinetics, the minor reaction pathways discussed in the preceding section produce UV-absorbing species, among them $CH_3C(O)O_2NO_2$, $CH_3O_2NO_2$, and HNO.

Spectra of the molecules expected to contribute to the overall UV absorbance of the reaction mixture are displayed in Figure 2. It is evident that, although these spectra are recognizably distinct, they overlap to a considerable extent. Therefore, some of these are combined in an effort to reduce the number of fitting parameters in eq 10 to a meaningful amount. The small contributions to the overall absorbance by NO and NO_2 are combined with the spectrum of methylnitrite as $\sigma_{CH_3ONO} - 3\sigma_{NO} + 2\sigma_{NO_2}$, reflecting the fact that three molecules of NO are lost and two of NO_2 generated for each molecule of CH_3ONO. Second, $CH_3C(O)O_2NO_2$ is omitted from the fitting procedure. Instead, the concentration nominally determined for $CH_3O_2NO_2$ is interpreted as representing the total peroxynitrate yield, since the spectra of $CH_3O_2NO_2$ and $CH_3C(O)O_2NO_2$ are very similar. Finally, HNO is omitted from the fitting procedure. The contribution of this channel to reaction (6) is approximately 10%.[13] The small amount of HNO formed is assumed to

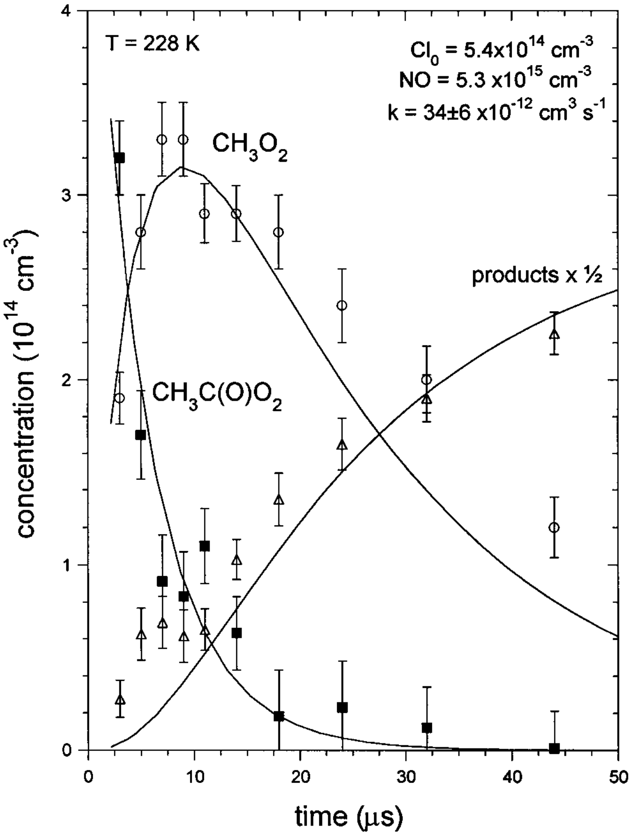

Figure 3. Concentration versus time profiles obtained from fitting the time-resolved absorbances of Figure 1 to the reference spectra of Figure 2 (see text). The solid lines display the simultaneous best fit of the data to the reaction model of Table 1, treating k_1 and the scaling of "products" as fitting parameters.

contribute primarily to the peroxynitrate yield owing to the significant overlap of its spectrum with those of the latter compounds.

The time-resolved spectra are fit via eq 10 to four reference spectra: those of $CH_3C(O)O_2$, CH_3O_2, the CH_3ONO combination, and the peroxynitrate products. Modifying the procedure used above to combine spectral contributions, e.g., omitting NO from the CH_3ONO composite, has little effect on the concentrations of $CH_3C(O)O_2$ and CH_3O_2 determined by the fitting procedure, a small effect on [CH_3ONO], and a medium effect on the apparent peroxynitrate yield. Because of the uncertainties in the secondary chemistry and those introduced by the lumping of reference spectra, the CH_3ONO and peroxynitrate yields were summed into an overall secondary product category. Figure 3 displays the results, showing the decay of $CH_3C(O)O_2$, the rise and fall of CH_3O_2, and the net product accumulation.

For each UV experiment, the three time versus concentration profiles are fit simultaneously to the reaction model of Table 1. Nominally, the only fitting parameter is k_1, the rate constant for the $CH_3C(O)O_2$ + NO reaction under investigation. Fitting three concentration dependences with a single free parameter represents an over constrained system. Unfortunately, because of systematic errors such as the optical cross sections of the products or the manner in which they are combined, the absolute yield of the products is suspect; however, its relative variation with time is more reliable. Thus, a second adjustable parameter is introduced to scale the product yield, in order that the absolute magnitude does not give undue weight to the quality of fit, and hence the determination of k_1. The solid lines in Figure 3 provide examples of the fits that are obtained via this procedure. The resulting rate constants are listed in Table 2 and plotted as a function of temperature in Figure 5.

Errors in the UV measurements of k_1 arise primarily from signal noise (~15%), i.e., from uncertainties in extracting concentrations from the UV absorbances. Smaller errors of 7% and 8% respectively arise from the 10% uncertainties in the UV cross sections of $CH_3C(O)O_2$ and CH_3O_2. In spite of the considerable secondary chemistry that takes place, uncertainties in the rate constants used in the reaction model of Table 1 contribute relatively little to the error bars. This is primarily due to the excess of NO as compared to the radical concentration and the fact that the reaction under investigation is the first one of the series. Uncertainties of 20% in the rate constants k_2, k_5, k_6, k_{11}, and k_{14} contribute <2% each to the overall error. Assuming that the individual uncertainties are statistically independent leads to an overall error of roughly ±20%.

c. IR Measurements. UV spectroscopy provides a means to probe two of the participants in the title reaction, $CH_3C(O)O_2$ and the product $CH_3C(O)O$, the latter being detected via the methylperoxy radical into which it is rapidly converted. A more complete investigation of this reaction is provided by IR probes of the other two participants, namely, NO and NO_2. Examples are presented in Figure 4 of transient IR absorption measurements that have been converted, via eq 9, into concentration versus time profiles. Consistent with expectations from the reaction mechanism, the quantity of NO consumed exceeds the NO_2 produced, which, in turn, is larger than the initial radical concentration. The ratios observed for $[Cl]_0:\Delta[NO]_\infty:[NO_2]_\infty$ are not quite the $1:-3:2$ expected from the principal reactions (1), (5), and (6) because of the additional minor reactions and because the initial NO concentration is not in large excess of the radical population.

The smooth curves in Figure 4 represent fits of the reaction model simultaneously to the NO and NO_2 data treating k_1 as an adjustable parameter. As with the UV fits described above, this represents an overconstrained system, particularly since the yield of NO_2 and the amount of NO consumed must be consistent with the initial radical population. The latter quantity is measured independently by substituting ethane for acetaldehyde, omitting NO, and measuring the amount of $C_2H_5O_2$ produced. The fact that both the NO and NO_2 traces are fit well adds confidence to the values obtained for k_1. Small apparently systematic deviations between the data and the fits arise primarily from systematic uncertainties in one or more of the quantities σ_{NO}, σ_{NO_2}, or $[Cl]_0$, which cannot be simultaneously accommodated by a model with a single degree of freedom. The fact that the initial rise observed for NO_2 lags predictions may be caused by reaction (1) producing NO_2 with a non-Boltzmann distribution of vibrational excitation that is then rapidly relaxed by collisions with buffer gas.

The principal sources of error incurred in the IR determination of k_1 are associated with the fact that three reactions consume NO and the fact that two reactions produce NO_2. Thus, an uncertainty of 20% in k_5, the methylperoxy reaction with nitric oxide, translates into an error of 14% in k_1. Because the changes in [NO] and [NO_2] are considerably larger than $[Cl]_0$, k_1 is also sensitive to the uncertainty in this quantity; an uncertainty of 5% in $[Cl]_0$ contributes a 12% error to k_1. Additionally, 5% uncertainties in σ_{NO} and σ_{NO_2} contribute to k_1 errors of 13% and 6%, respectively. The net error, assuming the above uncertainties to be statistically independent and including a 5% error due to signal noise, amounts to about ±25%.

IV. Discussion

Figure 5 depicts the variation of the $CH_3C(O)O_2$ + NO rate constant with temperature. The UV and IR measurements provide consistent values for k_1, with both methods indicating

TABLE 2: Acetylperoxy + Nitric Oxide Rate Constants

		conditions					results
temp (K)	meas. method	CH_3CHO (Torr)	P_{tot} (Torr)	O_2 (Torr)	$[NO]_0$ ($\times10^{14}$ cm^{-3})	$[Cl]_0$ ($\times10^{14}$ cm^{-3})	k_1 ($\times10^{-11}$ cm^3 s^{-1})
228	UV	2.4	118	101	153	11	2.1 ± 0.6
228	UV	1.5	110	99	54	5.4	3.4 ± 0.6
232	IR	1.2	104	21	31	9.8	2.0 ± 0.5
232	IR	1.2	104	21	64	9.8	2.3 ± 0.6
232	IR	1.2	104	21	126	9.8	2.8 ± 0.7
253	IR	1.7	110	31	32	1.6	1.7 ± 0.3
253	IR	1.7	110	31	58	1.6	1.5 ± 0.4
253	UV	1.6	112	33	64	6.0	2.1 ± 0.5
271	IR	1.5	110	21	28	11.4	1.7 ± 0.4
271	IR	1.5	110	21	58	11.4	2.3 ± 0.6
271	IR	1.5	110	21	109	11.4	2.2 ± 0.6
295	IR	2.0	105	32	32	1.25	1.3 ± 0.3
295	IR	2.0	105	32	59	1.25	1.4 ± 0.3
295	UV	2.5	124	106	125	9.0	1.6 ± 0.4
323	IR	1.3	107	27	20	14	1.4 ± 0.3
323	IR	1.3	107	27	42	14	1.3 ± 0.3
323	IR	1.3	107	27	84	14	1.0 ± 0.25
354	IR	2.3	120	35	31	4.3	0.87 ± 0.16
354	IR	2.3	120	35	57	4.3	0.94 ± 0.16
354	IR	2.3	120	35	104	4.3	1.1 ± 0.19
353	UV	1.9	118	34	65	4.9	1.2 ± 0.3

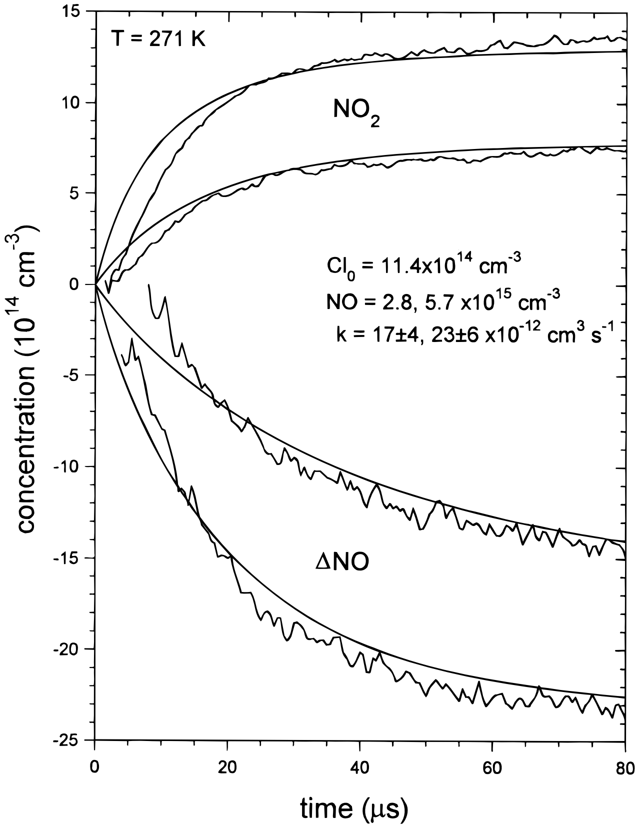

Figure 4. Concentration versus time profiles of NO loss and NO_2 generation following the photolysis of a $Cl_2/CH_3CHO/NO/O_2/N_2$ gas mixture as obtained via eq 9. The smooth lines represent fits of the data to the reaction model of Table 1, treating k_1 as an adjustable parameter.

a negative temperature dependence as is typical of peroxy radical reactions with nitric oxide. A fit of the combined data to the Arrhenius form yields $k_1 = (2.1^{+1.4}_{-0.8}) \times 10^{-12}e^{(570\pm140)/T}$ cm^3 s^{-1}. The present activation energy of −570 ± 140 K is very close to the value of −563 ± 115 K reported recently for the $CF_3C(O)O_2$ + NO reaction.[14] It is, however, ~1.7 times larger than the activation energy for a typical alkylperoxy reaction with NO; e.g., in the case of $C_2H_5O_2$ one finds that $E_a = -330 \pm 110$ K.[7]

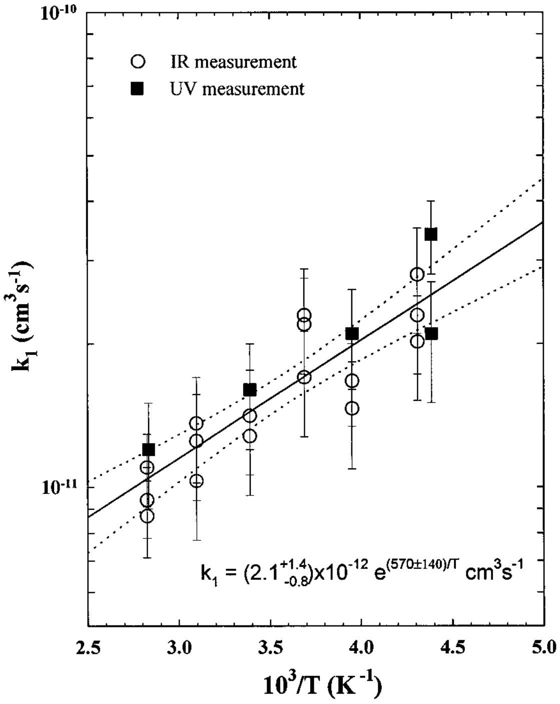

Figure 5. Temperature dependence of the $CH_3C(O)O_2$ + NO reaction rate constant. Error bars are $\pm2\sigma$ and include contributions from signal noise and from systematic uncertainties.

The present experiments show that the reaction of acetylperoxy with nitric oxide proceeds predominantly (>90%) via reaction (1); i.e., there is no evidence for the reaction channel

$$CH_3C(O)O_2 + NO + M \rightarrow CH_3C(O)ONO_2 + M \quad (18)$$

This assertion is supported by observations based on the levels of CH_3O_2 and NO_2 that are formed. If a second pathway, such as reaction (18), were present, it should manifest itself by showing reduced levels of both of these species. Instead, the rise in CH_3O_2, in particular its maximum level, is well fit by assuming that the reaction between $CH_3C(O)O_2$ and NO proceeds entirely via reaction (1). Furthermore, the observed NO_2 levels also require that a methylperoxy radical is formed for every acetylperoxy radical that is consumed, leaving little leeway for forming the adduct of reaction (18).

The room temperature rate constant, as obtained from the Arrhenius expression, is $k_1(295) = (1.4 \pm 0.2) \times 10^{-11}$ cm^3 s^{-1}. This is 25% smaller than the current recommended value[6] of 1.9×10^{-11} cm^3 s^{-1}; however, the recommendation is based on a determination relative to k_2 and has an estimated error of ±50%. The relative rate experiments of Cox and Roffey,[2] Hendry and Kenley,[5] Tuazon et al.,[4] and Krichner et al.[3] indicate that there is no significant temperature dependence to the ratio k_1/k_2. These measurements, however, cover only a small temperature range of about 290−325 K. A comparison of this ratio to values obtained from the present temperature-dependent measurements of k_1 and the literature values of k_2 depends on the parametrization that is employed to obtain the high-pressure limit in the latter case. If one combines, at $P_T = 760$ Torr, the high- and low-pressure limits from Bridier et al.,[15] $k_{2\infty} = 1.2 \times 10^{-11}(T/298)^{-0.9}$ cm^3 s^{-1}, $k_{20} = 2.7 \times 10^{-28}(T/298)^{-7.1}$ cm^6 s^{-1}, and a center broadening factor of $F_c = 0.3$ with our expression for k_1, then k_1/k_2 varies from 2.0 at 220 K to 1.3 at 355 K. This temperature variation is somewhat larger than might be expected from extrapolating the relative rate data. However, based on the reparametrization of k_2 listed in the JPL compilation of kinetic data for stratospheric modeling,[11] with $k_{2\infty} = 9.3 \times 10^{-12}(T/298)^{-1.5}$ cm^3 s^{-1}, $k_{20} = 9.7 \times 10^{-29}(T/298)^{-5.6}$ cm^6 s^{-1}, and $F_c = 0.6$, the ratio varies only from 2.0 at 220 K to 1.7 at 355 K.

The acetylperoxy radical plays a crucial role in both the formation and removal of PAN. At altitudes below about 7 km removal occurs primarily by thermal decomposition into $CH_3C(O)O_2$ and NO_2. It has been suggested by Stockwell et al.[16] that acetylperoxy chemistry can explain the recent observations of a strong diurnal variation in the $[O_3]/[PAN]$ ratio.[17,18] In order to test this hypothesis using atmospheric models, accurate rate constants are needed for the pertinent reactions. The current recommendation for k_1 is $(1.9 \pm 1.0) \times 10^{-11}$ cm^3 s^{-1} independent of temperature.[1,6] In contrast, the results of the present study show the $CH_3C(O)O_2 + NO$ rate constant to have a moderate negative temperature dependence. It remains to be seen how this modification, as well as the recent redeterminations[9,19] of the $CH_3C(O)O_2$ self-reaction and its reaction with CH_3O_2, influences model predictions of atmospheric PAN levels.

Note Added in Proof: Concurrent with the present study, Villalta and Howard [*J. Phys. Chem.*, submitted] have examined the $CH_3C(O)O_2 + NO$ reaction using a low-pressure flow reactor and found a temperature dependence significantly shallower than reported here.

References and Notes

(1) Lightfoot, P. D.; Cox, R. A.; Crowley, J. N.; Destriau, M.; Hayman, G. D.; Jenkin, M. E.; Moortgat, G. K.; Zabel, F. *Atmos. Environ.* **1992**, *26A*, 1805.

(2) Cox, R. A.; Roffey, M. J. *Environ. Sci. Technol.* **1977**, *11*, 900.

(3) Kirchner, F.; Zabel, F.; Becker, K. H. *Ber. Bunsen-Ges. Phys. Chem.* **1990**, *94*, 1379.

(4) Tuazon, E. C.; Carter, W. P. L.; Atkinson, R. *J. Phys. Chem.* **1991**, *95*, 2434.

(5) Hendry, D. G.; Kenley, R. A. *J. Am. Chem. Soc.* **1977**, *99*, 3198.

(6) Wallington, T. J.; Dagaut, P.; Kurylo, M. J. *Chem. Rev.* **1992**, *92*, 667.

(7) Maricq, M. M.; Szente, J. J., preceding paper in this issue.

(8) Atkinson, R.; Baulch, D. L.; Cox, R. A.; Hampson, R. F.; Kerr, J. A.; Troe, J. *J. Phys. Chem. Ref. Data* **1992**, *21*, 1125.

(9) Maricq, M. M.; Szente, J. J. *J. Phys. Chem.* **1996**, *100*, 4507.

(10) Maricq, M. M.; Wallington, T. J. *J. Phys. Chem.* **1992**, *96*, 986.

(11) DeMore, W. B.; Sander, S. P.; Golden, D. M.; Hampson, R. F.; Kurylo, M. J.; Howard, C. J.; Ravishankara, A. R.; Kolb, C. E.; Molina, M. J. *Chemical Kinetics and Photochemical Data for Use in Stratospheric Modeling*; JPL Publication 94-26, 1994.

(12) Mallard, W. G.; Westlely, F.; Herron, J. T.; Hampson, R. F. *NIST Chemical Kinetics Database Version 6.0*; NIST Standard Reference Data: Gaithersburg, MD, 1994.

(13) Frost, M. J.; Smith, I. W. M. *J. Chem. Soc., Faraday Trans.* **1990**, *86*, 1757.

(14) Maricq, M. M.; Szente, J. J. *J. Phys. Chem.* **1996**, *100*, 4514.

(15) Bridier, I.; Caralp, F.; Loirat, H.; Lesclaux, R.; Veyret, B.; Becker, K. H.; Reimer, A.; Zabel, F. *J. Phys. Chem.* **1991**, *95*, 3594.

(16) Stockwell, W. R.; Milford, J. B.; Gao, D.; Yang, Y.-J. *Atmos. Environ.* **1995**, *29*, 1591.

(17) Hartsell, B. E.; Aneja, V. P.; Lonneman, W. A. *J. Geophys. Res.* **1994**, *99*, 21033.

(18) Shepson, P. B.; Hastie, D. R.; So, K. W.; Schiff, H. I.; Wong, P. *Atmos. Environ.* **1992**, *26A*, 1259.

(19) Roehl, C. M.; Bauer, D.; Moortgat, G. K. *J. Phys. Chem.* **1996**, *100*, 4038.

JP960792C